0888-8809/08/$15.00/0
Printed in U.S.A.

Molecular Endocrinology 22(1):156–166

doi: 10.1210/me.2007-0274

Altered Selectivity of Parathyroid Hormone (PTH) and PTH-Related Protein (PTHrP) for Distinct Conformations of the PTH/PTHrP Receptor

Thomas Dean, Jean-Pierre Vilardaga, John T. Potts, Jr., and Thomas J. Gardella

Endocrine Unit (T.D., J.-P.V., J.T.P., T.J.G.) and Program in Membrane Biology (J.-P.V.), Massachusetts General Hospital and Harvard Medical School, Boston, Massachusetts 02114

PTH and PTHrP use the same G protein-coupled receptor, the PTH/PTHrP receptor (PTHR), to mediate their distinct biological actions. The extent to which the mechanisms by which the two ligands bind to the PTHR differ is unclear. We examined this question using several pharmacological and biophysical approaches. Kinetic dissociation and equilibrium binding assays revealed that the binding of [^{125}I]PTHrP(1–36) to the PTHR was more sensitive to GTPγS (added to functionally uncouple PTHR-G protein complexes) than was the binding of [^{125}I]PTH(1–34) (~75% maximal inhibition *vs.* ~20%). Fluorescence resonance energy transfer-based kinetic analyses revealed that PTHrP(1–36) bound to the PTHR more slowly and dissociated from it more rapidly than did PTH(1–34). The cAMP signaling response capacity of PTHrP(1–36) in cells decayed more rapidly than did that of PTH(1–34) ($t_{1/2}$ = ~1 *vs.* ~2 h). Divergent residue 5 in the ligand, Ile in PTH and His in PTHrP, was identified as a key determinant of the altered receptor-interaction responses exhibited by the two peptides. We conclude that whereas PTH and PTHrP bind similarly to the G protein-coupled PTHR conformation (RG), PTH has a greater capacity to bind to the G protein-uncoupled conformation (R^0) and, hence, can produce cumulatively greater signaling responses (via $R^0 \rightarrow RG$ isomerization) than can PTHrP. Such conformational selectivity may relate to the distinct modes by which PTH and PTHrP act biologically, endocrine *vs.* paracrine, and may help explain reported differences in the effects that the ligands have on calcium and bone metabolism when administered to humans. (*Molecular Endocrinology* 22: 156–166, 2008)

PTH AND PTHrP PLAY distinct biological roles yet act through the same G protein-coupled receptor (GPCR), the PTH/PTHrP receptor (PTHR). PTH is a gland-secreted endocrine hormone that regulates calcium and phosphate homeostasis by acting primarily on target cells in bone and kidney. Biosynthetic PTH(1–34) increases bone mineral density and bone strength in humans and indeed is now considered to be one of the most effective treatments for osteoporosis (1). PTHrP acts in a paracrine/autocrine fashion to regulate cell proliferation and differentiation programs in developing tissues (2). In addition, PTHrP appears to play a role in regulating bone remodeling in adults (3, 4).

PTH and PTHrP are most homologous in their amino-terminal (1–14) signaling domains (eight amino acid identities), and show moderate homology in their 14–34 binding domains (three identities). It has generally been inferred that the fully active (1–34) portions of PTH and PTHrP interact with the PTHR via largely identical mechanisms (5, 6). This mechanism is thought to consist of two principal components: an interaction between the C-terminal, binding domain of the ligand and the amino-terminal extracellular (N) domain of the receptor and an interaction between the amino-terminal, signaling domain of the ligand and the juxtamembrane (J) region of the receptor, which contains the extracellular loops and seven transmembrane helices (7–11). However, the extent, if any, to which the binding mechanisms used by the two ligands differ remains to be determined.

Interestingly, a recent series of clinical studies has revealed potential differences in the mechanisms by which PTH and PTHrP peptides function *in vivo*. Thus, PTHrP(1–36) was shown to increase bone mineral density to approximately the same extent as did PTH(1–34) but did not stimulate adverse bone-resorptive and hypercalcemic responses to the same extent as did PTH(1–34) (12–14). That such a difference is not due merely to a difference in pharmacokinetics is suggested by a direct comparison of the two peptides by steady-state infusions methods, which showed that PTHrP(1–36) is markedly less efficacious than PTH(1–34) for stimulating the renal synthesis of 1,25-$(OH)_2$ vitamin D_3 (13). Such results in humans could involve

First Published Online September 13, 2007

Abbreviations: Aib, α-Aminoisobutyric acid; CFP, cyan-fluorescent protein; FRET, fluorescent resonance energy transfer; Gα_SND, negative-dominant derivative of the stimulatory G protein α-subunit; IBMX, 3-isobutyl-1-methylxanthine; IP, inositol phosphate; PTHR, PTH/PTHrP receptor; YFP, yellow-fluorescent protein.

***Molecular Endocrinology* is published monthly by The Endocrine Society (http://www.endo-society.org), the foremost professional society serving the endocrine community.**

different mechanisms of action of the two ligands at the PTHR.

Here we explored more closely the mechanisms by which PTH and PTHrP interact with the PTHR. We focused particularly on the capacity of the two ligands to bind to different PTHR conformations. Of interest were two high-affinity conformations of the PTHR that can be distinguished based on their differing sensitivities to the nonhydrolyzable GTP analog GTPγS that can be observed in radioligand binding assays (7, 15, 16). One conformation, termed RG, is sensitive to GTPγS and is thus presumably coupled to a heterotrimeric G protein; the other, termed R^0 (17), is insensitive to GTPγS and is thus functionally uncoupled from G protein (16). The following schema describes the working hypothesis regarding the PTH-PTHR binding mechanism and associated changes in receptor conformation that underlies our work: $L+R \leftrightarrow LR_N \leftrightarrow LR^0_{NJ} \leftrightarrow LR_{NJ}G$, where L is ligand, R is receptor, LR_N is a low-affinity complex involving ligand interactions only to the PTHR N domain, LR^0_{NJ} is a high-affinity complex involving ligand interactions to both the N and J domains of the receptor, and $LR_{NJ}G$ is a high-affinity complex that is coupled to a heterotrimeric G protein (7, 16). One prediction of this schema is that different PTHR ligands could have different capacities to stabilize the R^0 conformation, due to differences in their mode of interaction with the N and/or J domains of the receptor. We further hypothesize that R^0 is an intermediary between the classical R and RG states of the two-state or ternary complex models of GPCR action (18, 19) and, as such, is a preactive receptor state that is primed to interact efficiently with a cognate heterotrimeric G protein. A prediction of this hypothesis is that the affinity with which a ligand binds to R^0 will be a determinant, in part, of the overall signaling response capacity of that ligand.

We explored these hypotheses specifically for PTH(1–34) and PTHrP(1–36) ligands. The results suggest the two ligands indeed differ in their capacities to stabilize R^0, in that PTHrP(1–36) binds more weakly to this conformation than does PTH(1–34). We show that this difference in conformational selectivity can result in different biological outcomes in cells, in terms of the cumulative signaling response produced, and is determined strongly by the amino acid divergence at position 5 in the ligands.

RESULTS

We first performed kinetic dissociation experiments to examine the stability of complexes formed between PTH and PTHrP radioligand analogs and the human PTHR stably expressed in membranes prepared from HKRK-B7 cells. For each radioligand, dissociation was examined in the presence and absence of GTPγS, so as to assess the effects of functionally uncoupling the receptor from heterotrimeric G proteins (Fig. 1). For [^{125}I]PTH(1–34) (Fig. 1A), the dissociation data, both in the absence and presence of GTPγS, were better fit by a two-phase decay equation than by a single-phase equation. In the absence of GTPγS (solid symbols), 17% of the complexes were unstable and decayed rapidly ($t_{1/2} < 1$ min), whereas the remaining 83% were stable and decayed much more slowly ($t_{1/2} \sim 4$ h). Upon addition of GTPγS (open symbols), the fraction of unstable complexes increased to 21%, such that

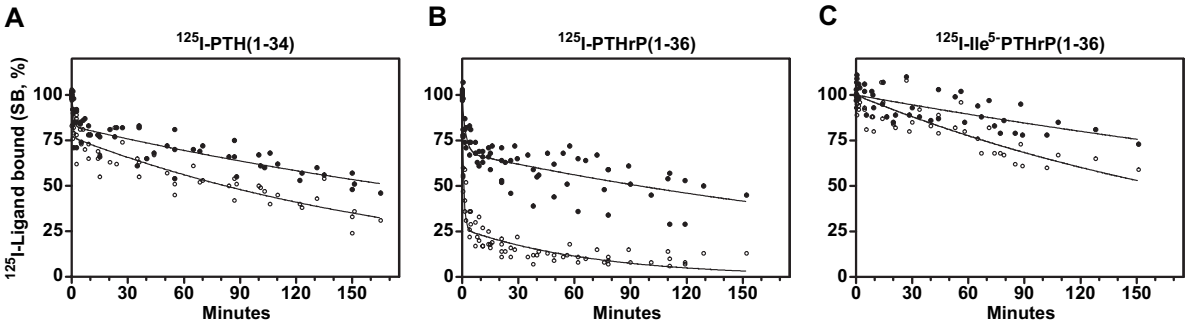

Fig. 1. Dissociation of PTH and PTHrP Ligands from the PTH Receptor and Effects of GTPγS

The radioligands [^{125}I][Nle^{8,21},Tyr^{34}]rPTH(1–34)NH_2 (A), [^{125}I][Tyr^{36}]PTHrP(1–36)NH_2 (B), and [^{125}I][Ile^5,Tyr^{36}]PTHrP(1–36)NH_2 (C) were prebound to the human PTHR in membranes prepared from HKRK-B7 cells for 90 min; then dissociation was initiated (t = 0) by the addition of the homologous unlabeled analog (5×10^{-7} M), added either alone (●) or with GTPγS (5×10^{-5} M, ○). At each time point, aliquots were withdrawn and immediately processed by rapid vacuum filtration to separate bound from free radioactivity. Nonspecific binding was determined in tubes containing the homologous unlabeled ligand (5×10^{-7} M) during both the preincubation and dissociation phases. The specifically bound radioactivity (SB) at each time point is expressed as a percentage of the specific binding observed at t = 0. Shown are aggregate data from four (A), five (B), or three (C) experiments. For each tracer radioligand, the respective values (means ± SEM) of total radioactivity (counts per minute) added, total radioactivity bound at t = 0, and nonspecifically bound radioactivity (averaged over the time course of each experiment) were 26,754 ± 2,652, 12,964 ± 2,476, and 522 ± 42 for [^{125}I]PTH(1–34) (n = 4); 31,597 ± 1,679, 5,959 ± 492, and 262 ± 17 for [^{125}I]PTHrP(1–36) (n = 5); and 51,335 ± 10,516, 22,904 ± 5,365, and 1,332 ± 337 for [^{125}I]Ile^5-PTHrP(1–36) (n =3), respectively. Curves were fit to the data using either a two-phase (A and B) or a single-phase (C) exponential decay equation.

79% remained stable ($t_{1/2}$ = ~2 h). These findings agree closely with previous dissociation studies performed on this radioligand, and highlight the capacity of PTH(1–34) to bind to a high affinity PTHR conformation (R^0) that is functionally uncoupled from heterotrimeric G proteins by GTPγS (15, 16).

Biphasic kinetics were also observed for [^{125}I]PTHrP(1–36); however, where the complexes were again mostly stable in the absence of GTPγS (68% decayed with a $t_{1/2}$ of ~3 h), most became unstable upon addition of GTPγS (72% decayed with a $t_{1/2}$ of ~1 min; Fig. 1B). This strong, destabilizing effect that GTPγS had on the binding of [^{125}I]PTHrP(1–36) to the PTHR mirrors that observed previously for [^{125}I][α-aminoisobutyric acid (Aib)^{1,3},M]PTH(1–15) (16), and suggests that, like ^{125}I-[Aib^{1,3},M]PTH(1–15), ^{125}I-PTHrP(1–36) binds predominantly to a G protein-coupled receptor conformation (RG).

The divergent residues at position 5 in PTH and PTHrP (Ile and His, respectively) have been shown to play important roles in PTHR-binding affinity (7, 20) and PTHR-subtype selectivity (21, 22). We therefore examined the receptor-dissociation properties of [^{125}I]Ile^5-PTHrP(1–36), to see whether the His^5→Ile substitution altered complex stability. This radioligand dissociated from the receptor slowly and with monophasic kinetics, both in the presence and absence of GTPγS ($t_{1/2} \geq 2$ h; Fig. 1C). Thus, the His^5→Ile substitution markedly enhanced the stability with which PTHrP bound to the PTHR, in the G protein-coupled, and especially the G protein-uncoupled state.

Effects of GTPγS on Equilibrium Binding

We further assessed the effects of GTPγS on the binding of the above radioligands to the PTHR under approximate equilibrium conditions. The radioligands were thus incubated with cell membranes for 90 min in the absence or presence of varying concentrations of GTPγS. Figure 2A shows that the binding of [^{125}I]PTH(1–34) and [^{125}I]Ile^5-PTHrP(1–36) to the human PTHR in HKRK-B7 cell membranes was largely unaffected by GTPγS (≤~20% inhibition at 1×10^{-4} M GTPγS), whereas the binding of [^{125}I]PTHrP(1–36) was strongly inhibited by GTPγS (~70% inhibition at 1×10^{-7} M GTPγS; $IC_{50} = 1 \times 10^{-9}$ M).

We also assessed binding to the rat PTHR using membranes prepared from the rat osteoblastic cell line ROS17/2.8 (endogenous PTHR expression). As seen with the human PTHR (Fig. 2A), the binding of [^{125}I]Ile^5-PTHrP(1–36) to the rat PTHR was again largely insensitive to GTPγS (Fig. 2B). The binding of [^{125}I]PTH(1–34) to the rat PTHR appeared more sensitive to GTPγS than was its binding to the human PTHR (Fig. 2, A *vs.* B), although the majority of binding was still resistant

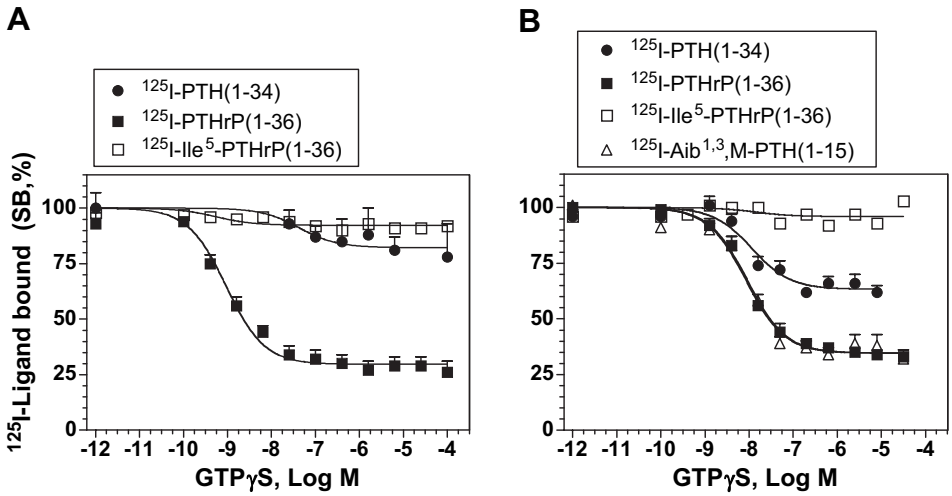

Fig. 2. GTPγS Sensitivity of PTH and PTHrP Ligand Binding to the Human and Rat PTHRs

Radioligand binding to the PTHR in membranes prepared from HKRK-B7 (A) or ROS 17/2.8 cells (B) was assessed under approximate equilibrium conditions in the presence of varying concentrations of GTPγS. Data are expressed as a percentage of the radioactivity specifically bound (SB) in the absence of GTPγS. The radioligands used were [^{125}I][Nle^{8,21},Tyr^{34}]PTH(1–34)NH_2, [^{125}I][Tyr^{36}]PTHrP(1–36)NH_2, [^{125}I][Ile^5,Tyr^{36}]PTHrP(1–36)NH_2, and [^{125}I][Aib^{1,3},Nle^8,Gln^{10},Har^{11},Ala^{12},Trp^{14},Tyr^{15}]hPTH(1–15)NH_2. Nonspecific binding was determined in wells containing the homologous unlabeled PTH or PTHrP ligand (5×10^{-7} M). In A, the values of total radioactivity (counts per minute) added, total radioactivity bound, and nonspecifically bound radioactivity were 21,045 ± 1,627, 2,806 ± 296, and 1,163 ± 325 for [^{125}I]PTH(1–34) (n =3); 27,489 ± 3,507, 3,164 ± 570, and 489 ± 85 for [^{125}I]PTHrP(1–36) (n =5); and 34,001 ± 711, 9,601 ± 959, and 569 ± 113 for [^{125}I]Ile^5-PTHrP(1–36) (n =5), respectively. In B, the corresponding values were 21,408 ± 1,245, 3,900 ± 170, and 1,214 ± 184 for [^{125}I]PTH(1–34) (n =6); 20,373 ± 951, 2,079 ± 211, and 467 ± 34 for [^{125}I]PTHrP(1–36) (n =6); 23,553 ± 891, 6,570 ± 1,142, and 1,040 ± 116 for [^{125}I]Ile^5-PTHrP(1–36) (n =6); and 30,986 ± 4,567, 847 ± 137, and 237 ± 27 for [^{125}I][Aib^{1,3},M]PTH(1–15) (n =6), respectively. Data are means (±SEM) from the number of experiments indicated by n, each performed in duplicate. Note that we have shown previously that GTPγS inhibits the binding of the [^{125}I][Aib^{1,3},M]PTH(1–15) analog to HKRK-B7 cell membranes by 88% and with an IC_{50} of 2.9 nM (16).

to GTPγS. As with the human PTHR, the binding of [^{125}I]PTHrP(1–36) to the rat PTHR was strongly inhibited by GTPγS and was as sensitive to GTPγS as was the binding of [^{125}I][Aib^{1,3},M]PTH(1–15) (Fig. 2B). These equilibrium binding data thus further suggest that although there are clearly differences among the different species of receptor, PTH(1–34) and Ile^5-PTHrP(1–36) bind more strongly to the G protein-uncoupled conformation of the PTHR, R^0, than do PTHrP(1–36) or [Aib^{1,3},M]PTH(1–15) and that the latter two peptides bind preferentially to the G protein-coupled conformation, RG.

Competition Analysis of R^0 and RG Binding Affinity

We then used competition methods to analyze the relative affinities with which PTH and PTHrP ligands bind to the RG and R^0 conformations of the PTHR. To assess binding to RG, we used [^{125}I][Aib^{1,3},M]PTH(1–15) as a tracer radioligand (binds predominantly to RG, see above) and membranes prepared from COS-7 cells cotransfected with the hPTHR and a negative-dominant $G\alpha_S$ subunit ($G\alpha_S$ND), which enriches for RG, *vs.* R or R^0, receptor conformations (16, 23, 24). To assess binding to R^0, we used [^{125}I]PTH(1–34) as a radioligand (binds predominantly to R^0) and membranes prepared from COS-7 cells transfected with the hPTHR alone; we also added GTPγS (1×10^{-5} M) to the binding reactions so as to functionally uncouple receptor-heterotrimeric G protein complexes and thus enrich for the R^0 (and R) conformations *vs.* RG. Comparison of the apparent affinities with which an unlabeled PTH or PTHrP ligand bound to the PTHR in these two assay formats would thus provide an assessment of the selectivity with which that ligand bound to the RG *vs.* R^0 conformation.

Figure 3A shows that PTH(1–34) bound to the R^0 conformation with a 4-fold weaker affinity than it did to the RG conformation (IC_{50} = 4.0 *vs.* 0.91 nM; P = 0.001; see R^0:RG ratio of Table 1). PTHrP(1–36) bound to R^0 with a 66-fold weaker affinity than it did to RG (28 *vs.* 0.42 nM; P = 0.04; Fig. 3B). PTHrP(1–36) was thus approximately 16-fold more selective for the RG conformation *vs.* R^0 than was PTH(1–34). Reciprocal exchange of residue 5 in these ligands reversed the pattern of conformational selectivity. Thus, His^5-PTH(1–34) bound to R^0 with a 670-fold weaker affinity than it did to RG (P = 0.01), whereas Ile^5-PTHrP(1–36) bound to R^0 with only a 3-fold weaker affinity than it did to RG (P = 0.0004; Fig. 3, C and D, and Table 1). The His^5-PTH(1–34) analog was therefore approximately 220-fold more selective for the RG conformation than was the Ile^5-PTHrP(1–36) analog.

We also assessed the effects of the Ile^5→His substitution on the binding affinity of human PTH(1–34)NH_2 and rat PTH(1–34)NH_2 peptides that lacked the methionine^{8,21}→norleucine and Phe^{34}→Tyr substitutions of our control PTH(1–34) analog, [Nle^{8,21},Tyr^{34}] rat PTH(1–34)NH_2, and thus contained only native rat or human PTH residues. We also assessed a human PTHrP(1–36)NH_2 peptide that lacked the Ile^{36}→Tyr substitution our control PTHrP(1–36) peptide, [Tyr^{36}]hPTHrP(1–36)NH_2. The resulting competition binding data (supplemental Fig. 1, published as supplemental data on The Endocrine Society's Journals Online web site at http://mend.endojournals.org; Table 1) revealed R^0:RG selectivity profiles that closely mirrored those obtained for the corresponding PTH and PTHrP control peptides. The results thus support the view that whereas both PTH(1–34) and PTHrP(1–36) bind well to the RG receptor conformation of the PTHR, PTH(1–34) binds with higher affinity to the R^0 conformation than does PTHrP(1–36) and that residue 5 in the ligand plays a key role in modulating this conformational selectivity. We note, however, that residues C-terminal of position 15 in PTH(1–34) are also likely to contribute to the capacity of the ligand to bind strongly to R^0, because

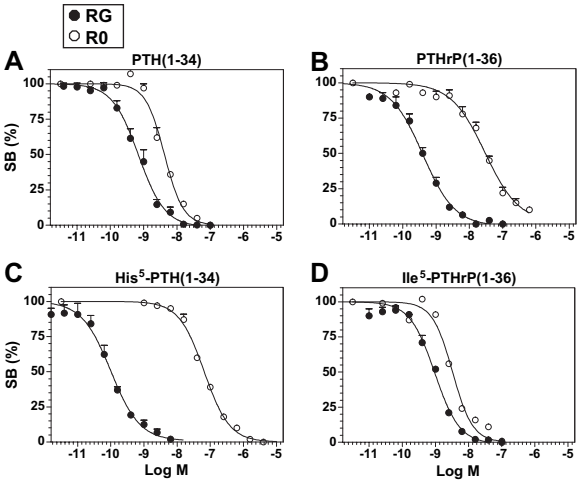

Fig. 3. Binding of PTH and PTHrP Analogs to the G Protein-Coupled and G Protein-Uncoupled PTHR Conformations

The binding of unlabeled PTH and PTHrP analogs to the G protein-coupled PTHR conformation (RG) and G protein-uncoupled PTHR conformation (R^0) was assessed by competition methods using membranes prepared from transiently transfected COS-7 cells. Binding to RG was assessed using membranes prepared from cells cotransfected with the hPTHR and a negative-dominant Gαs subunit, and [^{125}I][Aib^{1,3},Nle^8,Gln^{10},Har^{11},Ala^{12},Trp^{14},Tyr^{15}]hPTH(1–15)NH_2 as a tracer radioligand. Binding to R^0 was assessed using membranes prepared from cells transfected with the hPTHR alone, [^{125}I][Nle^{8,21},Tyr^{34}]rPTH(1–34)NH_2 as a tracer radioligand, and adding GTPγS to the reactions. The unlabeled ligands used were [Nle^{8,21},Tyr^{34}]rPTH(1–34)NH_2 (A); [Tyr^{36}]hPTHrP(1–36)NH_2 (B); [His^5,Nle^{8,21},Tyr^{34}]rPTH(1–34)NH_2 (C); and [Ile^5,Tyr^{36}]hPTHrP(1–36)NH_2 (D). Each curve shows data (mean ± SEM) from three to six experiments, each performed in duplicate (also see Table 1). Fifteen experiments were performed for each radioligand, for which the mean values of total radioactivity (counts per minute) added, total radioactivity bound, and nonspecifically bound radioactivity were 30,059 ± 2,263, 3,495 ± 417, and 398 ± 37 for [^{125}I]PTH(1–34) and 24,277 ± 2,022, 4,539 ± 848, and 236 ± 33 for [^{125}I][Aib^{1,3},M]PTH(1–15), respectively.

Table 1. Competition Binding to the RG and R^0 Conformations of the Human PTHR

	IC_{50} (nM)				
	RG [^{125}I]PTH(1–15) + GSND	n	R0 [^{125}I]PTH(1–34) + GTPγS	n	R^0:RG
[Nle^{8,21},Tyr^{34}]rPTH(1–34)NH_2	0.91 ± 0.28	6	4.0 ± 0.6	6	4
[His^5,Nle^{8,21},Tyr^{34}]rPTH(1–34)NH_2	0.10 ± 0.03	3	67 ± 8	3	670
[Tyr^{36}]hPTHrP(1–36)NH_2	0.42 ± 0.09	3	28 ± 6	3	66
[Ile^5,Tyr^{36}]hPTHrP(1–36)NH_2	0.92 ± 0.07	3	2.9 ± 0.1	3	3
rPTH(1–34)NH_2	0.34 ± 0.16	3	2.3 ± 0.3	3	7
[His^5]rPTH(1–34)NH_2	0.19 ± 0.04	5	26 ± 5	5	138
hPTH(1–34)NH_2	0.39 ± 0.24	3	6.6 ± 2.4	3	17
[His^5]hPTH(1–34)NH_2	0.76 ± 0.04	5	122 ± 35	5	160
hPTHrP(1–36)NH_2	0.59 ± 0.02	3	24 ± 3	3	42
[Aib^{1,3},M]rPTH(1–15)NH_2	0.74 ± 0.18	3	1029 ± 148	3	1397

[Aib^{1,3},M]PTH(1–15), which contains isoleucine at position 5, bound only weakly to R^0, while exhibiting strong affinity for RG (supplemental Fig. 1C; Table 1).

Direct Recording of PTHR Activation

The fluorescent resonance energy transfer (FRET) approach has recently been used to assess, in real time and in intact cells, the processes of ligand binding and receptor activation used by the PTHR (8, 25). We thus used this approach as an independent means to compare the time courses by which PTH and PTHrP ligands interact with the PTHR. The approach exploits an intramolecular FRET signal that occurs in a PTHR construct, PTHR-CFP_{IC3}/YFP_{CT}, that contains cyan-fluorescent protein (CFP) in the third intracellular loop and yellow-fluorescent protein (YFP) in the C-tail (25). The FRET signal produced by PTHR-CFP_{IC3}/YFP_{CT} occurs in the basal state and diminishes upon agonist binding, presumably due to conformational changes associated with receptor activation (25).

As shown in Fig. 4A, addition of hPTH(1–34) to cells expressing PTHR-CFP_{IC3}/YFP_{CT} induced a rapid ($t_{1/2}$ = 0.7 sec) reduction (~13%) in the FRET signal. The FRET signal remained suppressed during the 15 sec of ligand application (marked by the *black horizontal line* above the graphs in Fig. 4) and for at least 60 sec after the ligand-containing buffer was exchanged for a ligand-free buffer. This FRET response profile obtained for hPTH(1–34) replicates that observed for this ligand previously (25). The N-terminal peptide, [Aib^{1,3},M]PTH(1–14), induced a FRET response with slightly faster kinetics ($t_{1/2}$ = 0.5 sec) and with a shallower magnitude (~5%) than did hPTH(1–34) (Fig. 4B). Moreover, the FRET response produced by [Aib^{1,3},M]PTH(1–14) began to decay immediately upon exchange of the buffer to a ligand-free one (Fig. 4B). PTHrP(1–36) induced a relatively slow FRET response ($t_{1/2}$ = ~2–5 sec), and the signal began to decay immediately upon buffer exchange (Fig. 4C). Ile^5-PTHrP(1–36) induced a FRET response that was remarkably like that of PTH(1–34), with a rapid onset ($t_{1/2}$ = 0.5–0.7 sec) and very slow decay (Fig. 4D). These spectroscopic kinetic data are fully consistent with the data obtained in the above radioligand dissociation assays and thus support the hypothesis that PTH(1–34) and PTHrP(1–36) bind predominantly to distinct PTHR conformations and that ligand residue 5 plays a role in receptor conformation selectivity.

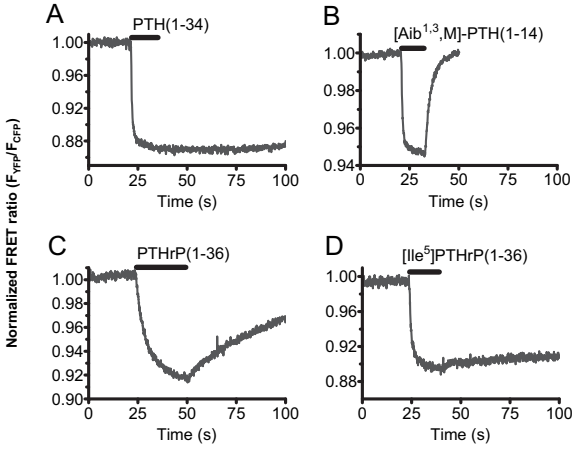

Fig. 4. FRET Analysis of Ligand Binding to the PTHR in HEK-293 Cells

HEK-PTHR-CFP_{IC3}/YFP_{CT} cells were used to assess the kinetics of ligand binding to and dissociation from the PTHR. In each *panel*, the trace shows the FRET ratio ($F_{YFP(535)}$/$F_{CFP(480)}$, normalized for channel spillover) obtained in cells superfused with buffer alone or with buffer containing a PTH peptide ligand (peptide additions indicated by *black bars* above each trace). The ligands used were hPTH(1–34) (A); [Aib^{1,3},Gln^{10},Har^{11},Ala^{12},Trp^{14}]hPTH(1–14)NH_2 (B); [Tyr^{36}]hPTHrP(1–36)NH_2 (C), and [Ile^5,Tyr^{36}]hPTHrP(1–36)NH_2 (D). Data are from a single experiment; identical results were obtained in at least three others.

Duration of cAMP Signaling Capacity

The data so far support the notion that certain PTH and PTHrP ligands can bind to a G protein-uncoupled form of the PTHR, R^0, with high affinity and thereby form a stable LR^0 complex. We next explored the hypothesis that this LR^0 complex could, over time, isomerize to LRG, and thus become active in terms of

cell signaling. Because this hypothesis predicts that a ligand that can bind stably to R^0 would have the capacity to produce a more prolonged signaling response than would a ligand that binds only weakly to R^0, we assessed the capacities of the ligands to stimulate cAMP production in PTHR-expressing cells at times after initially binding to the receptor. We thus treated cells with ligand at a relatively high concentration (100 or 300 nM) for 10 min, rinsed the cells thoroughly to remove unbound ligand, incubated the cells in buffer alone for various times, removed the buffer, and replaced it with a buffer containing the phosphodiesterase inhibitor 3-isobutyl-1-methylxanthine (IBMX), and after a 5-min incubation in IBMX, lysed the cells and measured intracellular cAMP. By this delayed cAMP protocol, only the intracellular cAMP generated during the 5-min IBMX phase would accumulate in the cells to measurable levels.

The experiments of Fig. 5A compare the time courses of the cAMP responses produced by PTHrP(1–36) and Ile^5-PTHrP(1–36) in HKRK-B7 cells. Immediately after the wash-out step (t = 0), cells treated with either ligand produced approximately the same, near-maximal amount of cAMP (~100-fold above basal). Two hours later, the cells treated with Ile^5-PTHrP(1–36) were still producing a cAMP response, which was 50% of the initial response (Fig. 5A). In contrast, the cells treated with PTHrP(1–36)

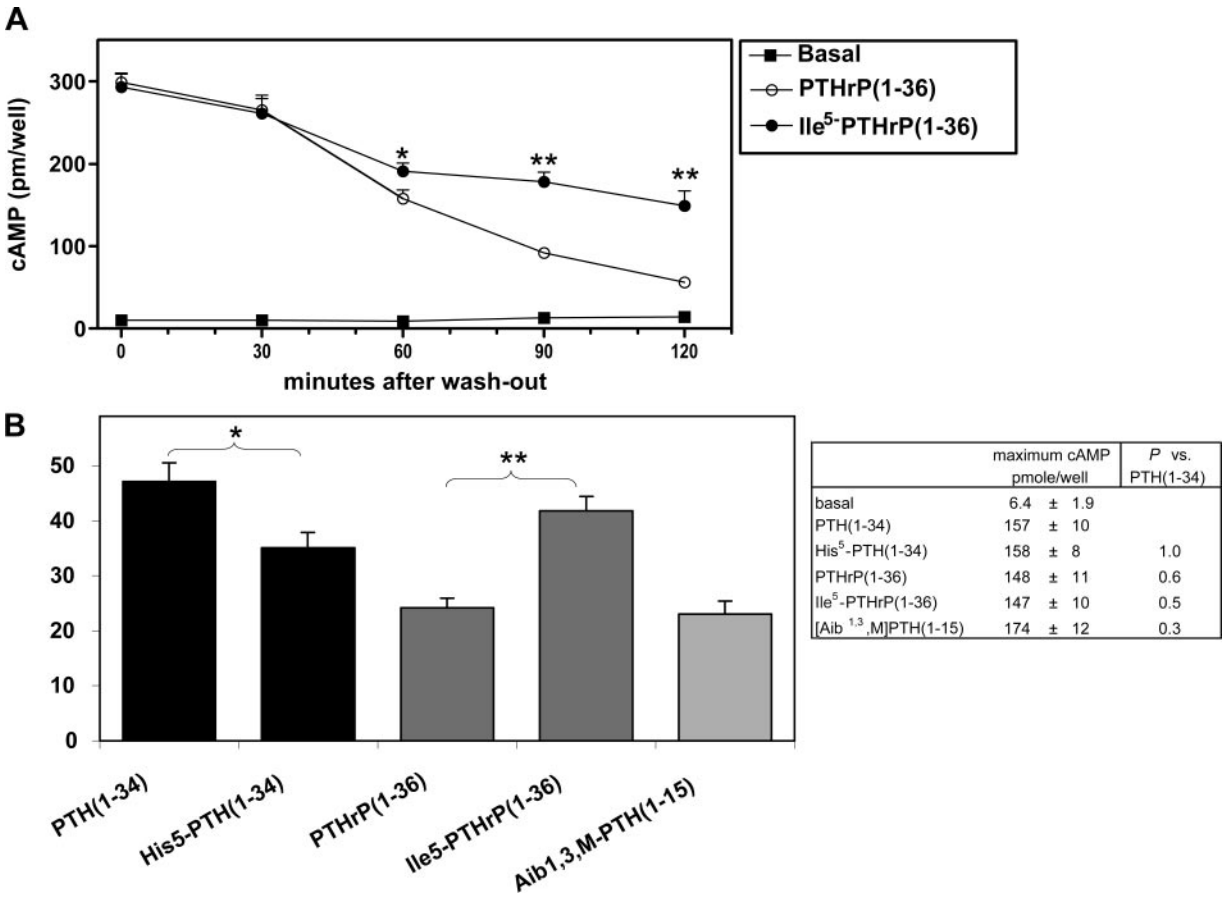

	maximum cAMP pmole/well	*P* vs. PTH(1-34)
basal	6.4 ± 1.9	
PTH(1-34)	157 ± 10	
His^5-PTH(1-34)	158 ± 8	1.0
PTHrP(1-36)	148 ± 11	0.6
Ile^5-PTHrP(1-36)	147 ± 10	0.5
[Aib ^{1,3},M]PTH(1-15)	174 ± 12	0.3

Fig. 5. Duration of cAMP-Signaling Responses Induced by PTH and PTHrP Analogs in Cells Stably Expressing the Human PTHR

The duration of cAMP signaling capacity of [Tyr^{36}]hPTHrP(1–36)NH_2 and [Ile^5,Tyr^{36}]hPTHrP(1–36)NH_2 was assessed by time-course experiments in HKRK-B7 cells (950,000 hPTHRs per cell, A). The cells were pretreated for 10 min with either buffer alone (basal) or buffer containing ligand (100 nM), washed (t = 0), incubated in buffer for the times indicated (washout phase), treated with IBMX for a final 5 min, and then assessed for intracellular cAMP accumulation. The response to each peptide observed by incubating cells concomitantly with peptide and IBMX for 10 min and omitting the was-out phase was 185 ± 16 and 198 ± 18 pmol/well for PTHrP(1–36) and Ile^5-PTHrP(1–36), respectively; the cAMP level in cells treated with IBMX in the absence of ligand was 2.0 ± 0.3 pmol/well. Data are means (±SEM) of three experiments, each performed in duplicate. In these experiments, [$Nle^{8,21}$,Tyr^{34}]rPTH(1–34)NH_2 was also analyzed and induced responses at each time point that were not different from those induced by [Ile^5,Tyr^{36}]hPTHrP(1–36)NH_2. Analogs were also assessed in HKRK-B64 cells (90,000 hPTHRs per cell, B). The cAMP was assessed 60 min after ligand washout, and the data are expressed as a percentile of the maximal cAMP response induced by each peptide (indicated in the *side panel*) in cells treated concomitantly with that ligand and IBMX for 10 min and omitting the washout phase. Data are means (±SEM) of four experiments, each performed in triplicate. *Asterisks* indicate statistical analyses of paired responses: PTHrP(1–36) *vs.* Ile^5-PTHrP(1–36) (A), or as indicated by *brackets* (B): *, $P < 0.05$; **, $P < 0.003$.

produced a signaling response at 2 h that was only 19% of the initial response, and thus about 65% less than that observed at 2 h for Ile^5-PTHrP(1–36) ($P < 0.003$). PTH(1–34) produced responses at each time point that were not significantly different from those produced by Ile^5-PTHrP(1–36) ($P > 0.05$, data not shown). Thus, the cAMP signaling responses induced by PTH(1–34) and Ile^5-PTHrP(1–36) decayed about twice as slowly as did that of PTHrP(1–36) ($t_{1/2} = \sim 2$ *vs.* ~ 1 h).

More prolonged responses for PTH(1–34) and Ile^5-PTHrP(1–36), relative to PTHrP(1–36), were also observed in ROS17/2.8 cells, which express the PTHR endogenously and at a relatively low level (70,000 per cell *vs.* 950,000 per cell for HKRK-B7 cells), as well as in HKRK-B64 cells, which stably express the hPTHR, also at a relatively low level (90,000 per cell) (supplemental Fig. 2, A and B).

Figure 5B compares the capacity of PTH or PTHrP ligands to produce a sustained cAMP signaling responses in HKRK-B64 cells at the 60-min time point. In these experiments, the cAMP response observed at 60 min after ligand washout is expressed as a percentile of the maximal cAMP response observed for that ligand (determined by treating cells concomitantly with that ligand and IBMX for 10 min and omitting the washout phase), as shown in the figure *inset*. At 60 min after washout, the cAMP responses generated by PTH(1–34) and Ile^5-PTHrP(1–36) were 47 and 40% of their corresponding maximal responses, respectively, whereas those of His^5-PTH(1–34) and PTHrP(1–36) were 34 and 19% of their maximal responses. The response induced by [Aib^{1,3},M]PTH(1–15) at 60 min was 23% of its maximum and thus comparable to that of PTHrP(1–36) ($P = 0.7$). Thus, in HKRK-B64 cells, PTH(1–34) and Ile^5-PTHrP(1–36) produce more sustained cAMP signaling responses than do PTHrP(1–36), His^5-PTH(1–34), and [Aib^{1,3},M]PTH(1–15).

In conventional cAMP dose-response assays performed in HKRK-B64 cells, little or no difference in potency or efficacy was observed for the analogs (supplemental Fig. 3A), whereas in ROS17/2.8 cells, a modest 4.5-fold reduction in cAMP signaling potency was observed for His^5-PTH(1–34), as compared with PTH(1–34) (supplemental Fig. 3B). No difference in inositol triphosphate signaling potency was observed for the analogs in COS-7 cells transiently transfected to express the hPTHR (supplemental Fig. 3C).

DISCUSSION

The studies presented here suggest intriguing differences in the mechanisms by which PTH and PTHrP interact with the PTH/PTHrP receptor, in that they point to differences in the capacities of the ligands to bind to and stabilize distinct receptor conformations. Our kinetic and equilibrium binding assays performed in cell membranes in the presence of GTPγS lead us to our main conclusion that whereas PTH(1–34) and PTHrP(1–36) bind with similar affinities to the G protein-coupled PTHR conformation, RG, PTH(1–34) binds with greater affinity to the G protein-uncoupled conformation, R^0, defined here as a receptor conformation that can bind ligand with high affinity in the presence of GTPγS (15–17).

In considering the potential biological implications for such differences in the capacity of PTH or PTHrP ligands to bind to different PTHR conformations, and in particular, R^0, we hypothesized that R^0, although not coupled to G protein, is a preactive state that is primed to interact efficiently with a G protein as it encounters one. Thus, the LR^0 complex, upon engaging a G protein, can isomerize to LRG and so become signaling competent. This hypothesis, in turn, predicts that a ligand that can bind stably to R^0 will have the potential to produce a biological signal at longer times after it initially binds to the receptor than will a ligand that binds only weakly to R^0. We performed the delayed cAMP time-course assays of Fig. 5 and supplemental Fig. 2 as means to test these hypotheses. The results showed that ligands that exhibited relatively high affinities for R^0 in the binding assays, PTH(1–34) and Ile^5-PTHrP(1–36), produced greater cAMP responses at times after initial binding than did ligands that bound more weakly to R^0, PTHrP(1–36) and His^5-PTH(1–34). The results thus support the hypothesis that PTH and PTHrP ligands exhibit different conformational selectivities for the PTHR and, more generally, support the notion that the capacity of a ligand to bind to R^0 can determine, in part, the overall signaling capacity of that ligand in target cells.

The capacity to produce a signaling response at times after initial binding of a ligand to its receptor could be biologically relevant in situations where the cognate G proteins are in low abundance, relative to the receptor, due, for example, to differences in expression levels and/or subcellular compartmentalization. It is also possible that formation of a stable LR^0 complex could enable multiple (catalytic) rounds of G protein activation (26, 27) and thereby contribute to signal amplification. In any event, our present data suggest that receptor conformational selectivity can be a factor that contributes to the functionality of a PTH receptor ligand, and this might be a property of the PTHR that can be exploited in ligand-design efforts. In this regard, we have recently developed a PTH analog, [Ala^{1,12},Aib^3,Gln^{10},Har^{11},Trp^{14},Arg^{19}]hPTH(1–28)NH_2, that binds to the R^0 conformation of the PTHR with considerably higher ($\sim$80-fold on the rat PTHR) affinity than does hPTH(1–34)NH_2 and, when injected into mice, produces biological responses (increases in serum calcium and suppression of serum phosphate) that are significantly more prolonged than those produced by PTH(1–34) (28, 29). These findings, which are not based on differing serum concentrations of the ligands, based on pharmacokinetic data, strongly suggest that the capacity of a ligand to bind to the R^0

conformation of the PTHR can contribute importantly to the biological response profile of that ligand.

Our acute dose-response signaling assays detected little if any difference in the potencies with which PTH(1–34) and PTHrP(1–36) ligands stimulate cAMP or inositol phosphate (IP) accumulation (supplemental Fig. 3; Table 2), results that, by themselves, are consistent with the view that the two ligands interact with the PTHR via largely similar mechanisms. The time-delayed cAMP assays of Fig. 5 (and supplemental Fig. 2) brought out previously unappreciated differences in the signaling properties of the two ligands, evident as differences in the signal output at times after initial binding of ligand to the receptor. Although these findings are consistent with a model involving altered selectivities for different PTHR conformations, we cannot, at present, exclude a possible role for differences in receptor desensitization mechanisms (30–33). The relationship between receptor conformational selectivity and such internalization/desensitization processes will be an interesting and important matter to explore in future studies.

The capacity of ligand to bind stably to LR^0 might also facilitate coupling to secondary G proteins that presumably have lower affinity for the ligand-receptor complex than does the primary G protein. For the PTHR, this could involve coupling to G proteins of the $G\alpha_{q/11}$, $G\alpha_{i/o}$, or $G\alpha_{12/13}$ subclasses, which have been shown to be activated by the PTHR in response to PTH(1–34). More studies are needed to assess the relationship between PTHR ligand conformational selectivity and activation of these other G protein signaling pathways. It is also interesting to note that some capacity to form a stable LR^0 complex might be an intrinsic property of the class B GPCRs, most if not all of which use a two-site ligand-binding mechanism involving interactions to both the N and J receptor domains. Thus, several others of these receptors, including the receptors for calcitonin (34), CRH (17), and glucagon (35) have been shown to form a stable complex with their cognate peptide ligand in the presence of a nonhydrolyzable guanine nucleotide analog.

We do not know whether differing capacities to bind to the R^0 state of the receptor explain any of the differences in pharmacological or physiological effects attributed to the two ligands, PTH and PTHrP. It has been of interest to speculate how two physiologically different systems, one paracrine/autocrine (PTHrP) and the other endocrine (PTH) can effectively use one common receptor, widely present in cells, yet produce different effects. PTHrP is produced locally with high regional concentrations likely (36), whereas PTH is secreted into the circulation. Stabilization or formation of distinctive PTHR conformations that differ in terms of duration of signaling could be one factor that underlies, in part, the different modes of action. For example, a shorter duration of signaling might be a useful mechanism for a paracrine factor involved in the timing of cell differentiation programs. PTHrP(1–36) peptide, in the limited human studies reported so far, does seem to differ from PTH(1–34) in the extent of hypercalcemia induced after a single sc injection (14), stimulation of 1,25-$(OH)_2$ vitamin D_3 production after iv infusion (13), and stimulation of bone resorption after several months of daily sc administration (12). The differences in the capacities of PTH and PTHrP ligands to bind to the R^0 conformation of the PTHR described herein could potentially explain some of these differing pharmacological properties of the ligands and may be of value to explore therapeutically.

MATERIALS AND METHODS

Peptides

Peptides used were as follows (abbreviated, full structural name): PTH(1–34), [$Nle^{8,21}$,Tyr^{34}]rat(r)PTH(1–34)NH_2; His^5-PTH(1–34), [His^5,$Nle^{8,21}$,Tyr^{34}]rPTH(1–34)NH_2; PTHrP(1–36), [Tyr^{36}]human(h)PTHrP(1–36)NH_2; Ile^5-PTHrP(1–36), [Ile^5,Tyr^{36}]hPTHrP(1–36)NH_2; [$Aib^{1,3}$,M]PTH(1–15), [$Aib^{1,3}$, Nle^8,Gln^{10},Har^{11},Ala^{12},Trp^{14},Tyr^{15}]rPTH(1–15)NH_2 (37); hPTH(1–34), hPTH(1–34)NH_2; His^5-hPTH(1–34) [His^5]-hPTH(1–34)NH_2; rPTH(1–34), (rPTH(1–34)NH_2; and His^5-rPTH(1–34), [His^5]ratPTH(1–34)NH_2. These peptides were synthesized by the Massachusetts General Hospital Biopolymer Core facility, as described (38). The human PTH(1–34) (free carboxy terminus) used in FRET analyses was purchased from Bachem California (Torrance, CA). Peptide quality was verified by analytical HPLC, matrix-assisted laser desorption/ionization mass spectrometry and amino acid analysis, and peptide concentrations of stock solutions were established by amino acid analysis.

Table 2. cAMP and IP Signaling Properties of PTH and PTHrP Ligands

	cAMP				IP	
	HKRK-B64 Cells[a]		ROS 17/2.8 Cells[b]		COS-7 Cells (hPTHR)[c]	
	EC_{50} (nM)	E_{max} (pmol/well)	EC_{50} (nM)	E_{max} (pmol/well)	EC_{50} (nM)	E_{max} (cpm/well)
[$Nle^{8,21}$,Tyr^{34}]rPTH(1–34)NH_2	5.1 ± 0.5	55 ± 12	0.60 ± 0.1	353 ± 54	18 ± 3	2407 ± 138
[His^5,$Nle^{8,21}$,Tyr^{34}]rPTH(1–34)NH_2	2.7 ± 0.6[g]	59 ± 12	2.8 ± 0.2[g]	398 ± 68	30 ± 12	2231 ± 229
[Tyr^{36}]hPTHrP(1–36)NH_2	5.6 ± 1.3	62 ± 15	0.78 ± 0.23	366 ± 43	23 ± 8	2514 ± 270
[Ile^5,Tyr^{36}]hPTHrP(1–36)NH_2	5.4 ± 1.9	61 ± 14	1.0 ± 0.6	355 ± 51	23 ± 7	2793 ± 303

[a] Data are means (±SEM) from four experiments; E_{max} for basal cAMP (not subtracted) was 5.2 ± 0.9 pmol/well.
[b] Data are means (±SEM) from three experiments; E_{max} for basal cAMP (not subtracted) was 21 ± 1 pmol/well.
[c] Data are means (±SEM) from five experiments; E_{max} for basal IP value (not subtracted) was 330 ± 8 cpm/well.
[d] *P vs.* [$Nle^{8,21}$,Tyr34]rPTH(1–34)NH_2 ≤ 0.02.

Radiolabeled peptide variants were prepared by the oxidative chloramine-T procedure using $Na^{125}I$ (specific activity, 2200 Ci/mmol; PerkinElmer/NEN Life Science Products, Boston, MA) and were purified by reversed-phase HPLC.

Cell Culture

Cells were cultured at 37 C in a humidified atmosphere containing 5% CO_2 in DMEM supplemented with 10% fetal bovine serum (HyClone, Logan UT), 100 U/ml penicillin G, and 100 μg/ml streptomycin sulfate (Invitrogen Corp., Carlsbad, CA). The PTHR-expressing cell lines used were HKRK-B7, HKRK-B64, ROS 17/2.8, and HEK-PTHR-CFP_{IC3}/YFP_{CT}. The HKRK-B7 and HKRK-B64 lines are derivatives of the porcine kidney cell line LLC-PK_1 and are stably transfected to express the human PTHR at approximate surface densities of 950,000 and 90,000 PTH-binding sites per cell, respectively (39). ROS 17/2.8 cells are rat osteosarcoma cells (40) and express the endogenous rat PTHR at an approximate surface density of 70,000 PTH-binding sites per cell (41). HEK-PTHR-CFP_{IC3}/YFP_{CT} cells are derived from HEK-293 cells and stably express PTHR-CFP_{IC3}/YFP_{CT}, a human PTHR construct previously called PTHR-Cam (25), that contains CFP inserted at Gly^{395} in the third intracellular loop and YFP inserted into the C-terminal tail. Cells were propagated in T75 flasks and divided into 24-well plates for assays with intact cells, six-well plates for membrane preparations, or onto glass coverslips for FRET studies.

COS-7 cells were transiently transfected using Fugene-6 (Roche Diagnostics, Indianapolis, IN) and CsCl-purified plasmid DNA (3 μl Fugene-6 per 1 μg DNA). The wells of six- and 24-well plates were transfected with 1 μg and 250 ng DNA per well, respectively. Cells were transfected with the PTHR alone or cotransfected with the PTHR and a negative-dominant $G\alpha_S$ subunit, $G\alpha_S$ND. This $G\alpha_S$ND subunit binds more effectively, but unproductively, to receptors than does wild-type $G\alpha_S$ (24) and thus enhances binding of [^{125}I][$Aib^{1,3}$,M]PTH(1–15)NH_2 radioligand to the PTHR in an RG conformation (see below) (23).

Binding Studies

Binding studies were performed using cell membranes as described (16). Reactions were incubated at room temperature in membrane assay buffer [20 mM HEPES (pH 7.4), 0.1 M NaCl, 3 mM $MgSO_4$, 20% glycerol, 3 mg/ml BSA, protease inhibitor cocktail, and, at final concentrations, 1 mM AEBSF, 0.8 μM aprotonin, 20 μM leupeptin, 40 μM bestatin, 15 μM pepstatin A, and 14 μM E-64; Sigma-Aldrich Inc., St. Louis, MO). Reactions contained a total membrane protein concentration of 20–100 μg/ml and a total radioactivity concentration of approximately 150,000 cpm/ml. Unlabeled peptide ligands and/or GTPγS (Sigma-Aldrich) were added to the reactions as indicated. At the end of the reaction, bound and free radioligand were separated by vacuum filtration using a 96-well vacuum filter plate and vacuum filter apparatus (Multi-Screen system with Durapore HV, 0.65-μm filters; Millipore Corp., Milford, MA); the air-dried filters were then detached from the plate and counted for γ-radioactivity using a γ-counter.

Radioligand Dissociation

These studies were performed as bulk reactions in 15-ml round-bottom polystyrene snap-cap tubes (Falcon) (total reaction volume = 5.0 ml). Membranes and radioligand were preincubated for 90 min to allow complex formation; the dissociation phase was then initiated by the addition of an excess of the unlabeled analog of the radioligand (5×10^{-7} M final concentration), with or without GTPγS (5×10^{-5} M). Immediately before this addition (t = 0), and at successive time points thereafter, 0.2-ml aliquots (~30,000 cpm) were withdrawn and immediately processed by vacuum filtration, as described above. Nonspecific binding was determined in parallel reaction tubes containing the unlabeled analog (5×10^{-7} M) in both the preincubation and dissociation phases. The specifically bound radioactivity at each time point was calculated as a percent of the radioactivity specifically bound at t = 0.

Equilibrium Competition Binding and GTPγS Inhibition

Binding reactions performed with [^{125}I][$Aib^{1,3}$,M]PTH(1–15) radioligand were assembled and incubated in the wells of the 96-well, Multi-Screen vacuum filtration plates. Membranes, tracer radioligand, and various concentrations of unlabeled ligands and/or GTPγS were incubated in the wells for 90 min, following which, the reaction plates were processed by rapid vacuum filtration, as described above. Binding reactions performed with [^{125}I]PTH(1–34) radioligand were assembled and incubated in 96-well polystyrene microtiter plates (Falcon, total reaction volume = 230 μl) and at the end of the incubation were transferred to the Multi-Screen vacuum filtration plates and processed, as described above. This transfer minimized nonspecific binding of [^{125}I]PTH(1–34) to the Multi-Screen filter membranes. For both radioligands, the nonspecific binding was determined in reactions containing a saturating concentration of the unlabeled analog of the radioligand. The specifically bound radioactivity was calculated as a percentage of the radioactivity specifically bound in the absence of a competing ligand or GTPγS.

To assess the binding of unlabeled peptide ligands to the G protein-uncoupled PTHR conformation (R^0), we used membranes prepared from COS-7 cells transiently transfected with the PTHR, [^{125}I]PTH(1–34), as a tracer radioligand and added GTPγS to the binding reactions (1×10^{-5} M final concentration). This binding format is based on the premise that [^{125}I]PTH(1–34) binds predominantly to the R^0 conformation of the PTHR and that this conformation is enriched in the membranes, relative to RG, by the presence of GTPγS (15, 16). A similar approach, using radiolabeled peptide agonist and GTPγS, was used by Hoare and colleagues (17) to assess binding to the R^0 conformation of the corticotropin-releasing factor receptor-1. To assess binding to the G protein-coupled conformation (RG), we used membranes prepared from cells cotransfected with the PTHR and a negative-dominant $G\alpha_S$ subunit ($G\alpha_S$ND), and we used [^{125}I][$Aib^{1,3}$,M]PTH(1–15) as a tracer radioligand. This binding format is based on the premise that [^{125}I][$Aib^{1,3}$,M]PTH(1–15) binds predominantly to the RG conformation of the PTHR and that this conformation is enriched in the membranes, relative to R or R^0, by the presence of $G\alpha_S$ND (7, 23, 24). We note that binding of a ligand to any low-affinity PTHR conformation (R) will not be detectable in these assays, given the low concentrations (~25 pM) of tracer radioligands used.

FRET

FRET analyses using HEK-PTHR-CFP_{IC3}/YFP_{CT} cells were performed as described (25). With PTHR-CFP_{IC3}/YFP_{CT}, excitation of the CFP donor with UV light ($\lambda_{max.ex.}$ = 436 nm; $\lambda_{max.em.}$ = 480 nm) produces an intramolecular FRET to the YFP acceptor, resulting in emission from that YFP ($\lambda_{max.ex.}$ = 480 nm, $\lambda_{max.em.}$ = 535 nm). This FRET response is observable as a decrease in intensity of CFP light emission at 480 nm and an increase in intensity of YFP light emission at 535 nm. The FRET signal occurs in the ground-state receptor and decreases upon binding of a PTH agonist ligand (25). PTH ligands were applied to and washed from the cells using a computer-assisted, solenoid valve-controlled, rapid superfusion device (ALA Scientific Instruments, Westbury, NY). Solution-exchange times were 5–10 msec. Fluorescence was monitored using a Zeiss inverted microscope equipped with a ×100 objective and a dual-emission photometric system

(Till Photonics, Planegg, Germany), coupled to an avalanche photodiode detection system and an analog-digital converter (Axon Instruments, Foster City, CA). The FRET signal detected upon excitation at 436 nm was calculated as a normalized FRET ratio: $F_{YFP(535nm)}/F_{CFP(480nm)}$, where $F_{YFP(535nm)}$ is the emission at 535 nm, corrected for spillover of the CFP signal into the YFP channel, and $F_{CFP(480nm)}$ is the emission at 480 nm, corrected for spillover (minimal) of the YFP emission into the CFP channel. Changes in fluorescence emissions due to photobleaching were subtracted.

Stimulation of Intracellular cAMP and Inositol Phosphate

Intracellular cAMP levels were measured by RIA (38). The capacity of a ligand to produce a delayed cAMP response in cells was assessed as follows (33, 42). The cells in 24-well plates were rinsed in binding buffer [50 mM Tris-HCl (pH 7.7), 100 mM NaCl, 5 mM KCl, 2 mM $CaCl_2$, 5% heat-inactivated horse serum, 0.5% heat-inactivated fetal bovine serum] and then incubated in binding buffer with or without a peptide ligand (1×10^{-7} or 3×10^{-7} M) for 10 min at room temperature. The cells were then washed with three changes of binding buffer and incubated further in binding buffer for varying times (1–120 min). Then, the buffer was replaced by binding buffer containing IBMX (2 mM), and after an additional 5-min incubation, the intracellular cAMP was quantified. By this approach, only the cAMP produced during the final IBMX stage of the incubation is measurable, because that produced before IBMX addition is degraded by cellular phosphodiesterases.

The stimulation of intracellular IPs was measured in transiently transfected COS-7 cells that were prelabeled (16 h) with [^{3}H]myo-D-inositol (2 μCi/ml) (38). Cells were treated with ligand in DMEM containing fetal bovine serum (10%) and LiCl (30 mM) for 30 min. The cells were then lysed with ice-cold, trichloroacetic acid (5%), and IPs were extracted from the acid-lysates by ion-exchange filtration.

Data Calculations

Data were processed using Microsoft Excel and GraphPad Prism 4.0 software packages. Dissociation time-course data were analyzed using a biexponential decay equation, except when an F test analysis indicated a monoexponential equation provided a better fit ($P\alpha > 0.02$). Data from equilibrium binding, cAMP, and IP dose-response assays were analyzed using a sigmoid dose-response equation with variable slope, which yielded values of EC_{50}, IC_{50} (concentration of ligand producing the half-maximal effect), and E_{max} (maximal cAMP or IP response). Paired data sets were statistically compared using the Student's *t* test (two tailed) assuming unequal variances for the two sets.

Acknowledgments

We thank Catherine Berlot (Weis Center for Research, Danville, PA) for providing the $G\alpha_S$ND expression plasmid.

Received May 29, 2007. Accepted September 7, 2007.

Address all correspondence and requests for reprints to: Thomas J. Gardella, Endocrine Unit, Massachusetts General Hospital, Boston, Massachusetts 02114. E-mail: Gardella@helix.mgh.harvard.edu.

This work was supported by Grant DK-11794 from the National Institutes of Health.

Disclosure Statement: T.D. and J.-P.V have nothing to declare. T.J.G. and J.T.P. are recipients of a research grant from Chugai Pharmaceutical Co. of Japan; the grant is for the study of PTH ligands.

REFERENCES

1. Tashjian Jr AH, Gagel RF 2006 Teriparatide [human PTH(1–34)]: 2.5 years of experience on the use and safety of the drug for the treatment of osteoporosis. J Bone Miner Res 21:354–365
2. Kronenberg HM 2006 PTHrP and skeletal development. Ann NY Acad Sci 1068:1–13
3. Miao D, He B, Jiang Y, Kobayashi T, Soroceanu MA, Zhao J, Su H, Tong X, Amizuka N, Gupta A, Genant HK, Kronenberg HM, Goltzman D, Karaplis AC 2005 Osteoblast-derived PTHrP is a potent endogenous bone anabolic agent that modifies the therapeutic efficacy of administered PTH 1–34. J Clin Invest 115:2402–2411
4. Martin TJ 2005 Osteoblast-derived PTHrP is a physiological regulator of bone formation. J Clin Invest 115: 2322–2324
5. Caulfield MP, McKee RL, Goldman ME, Duong LT, Fisher JE, Gay CT, DeHaven PA, Levy JJ, Roubini E, Nutt RF, Chorev M, Rosenblatt M 1990 The bovine renal parathyroid hormone (PTH) receptor has equal affinity for two different amino acid sequences: the receptor binding domains of PTH and PTH-related protein are located within the 14–34 region. Endocrinology 127:83–87
6. Abou-Samra A-B, Uneno S, Jüppner H, Keutmann HT, Potts JT, Jr., Segre GV, Nussbaum SR 1989 Non-homologous sequences of parathyroid hormone and the parathyroid hormone related peptide bind to a common receptor on ROS 17/2.8 cells. Endocrinology 125: 2215–2217
7. Hoare S, Gardella T, Usdin T 2001 Evaluating the signal transduction mechanism of the parathyroid hormone 1 receptor: effect of receptor-G-protein interaction on the ligand binding mechanism and receptor conformation. J Biol Chem 276:7741–7753
8. Castro M, Nikolaev VO, Palm D, Lohse MJ, Vilardaga JP 2005 Turn-on switch in parathyroid hormone receptor by a two-step parathyroid hormone binding mechanism. Proc Natl Acad Sci USA 102:16084–16089
9. Wittelsberger A, Corich M, Thomas BE, Lee BK, Barazza A, Czodrowski P, Mierke DF, Chorev M, Rosenblatt M 2006 The mid-region of parathyroid hormone (1–34) serves as a functional docking domain in receptor activation. Biochemistry 45:2027–2034
10. Shimizu N, Dean T, Tsang JC, Khatri A, Potts Jr JT, Gardella TJ 2005 Novel parathyroid hormone (PTH) antagonists that bind to the juxtamembrane portion of the PTH/PTH-related protein receptor. J Biol Chem 280: 1797–1807
11. Gensure RC, Gardella TJ, Juppner H 2005 Parathyroid hormone and parathyroid hormone-related peptide, and their receptors. Biochem Biophys Res Commun 328: 666–678
12. Horwitz MJ, Tedesco MB, Gundberg C, Garcia-Ocana A, Stewart AF 2003 Short-term, high-dose parathyroid hormone-related protein as a skeletal anabolic agent for the treatment of postmenopausal osteoporosis. J Clin Endocrinol Metab 88:569–575
13. Horwitz MJ, Tedesco MB, Sereika SM, Syed MA, Garcia-Ocana A, Bisello A, Hollis BW, Rosen CJ, Wysolmerski JJ, Dann P, Gundberg C, Stewart AF 2005 Continuous PTH and PTHrP infusion causes suppression of bone formation and discordant effects on $1,25(OH)_2$ vitamin D. J Bone Miner Res 20:1792–1803
14. Horwitz MJ, Tedesco MB, Sereika SM, Garcia-Ocana A, Bisello A, Hollis BW, Gundberg C, Stewart AF 2006 Safety and tolerability of subcutaneous PTHrP(1–36) in healthy human volunteers: a dose escalation study. Osteoporos Int 17:225–230
15. Hoare S, de Vries G, Usdin T 1999 Measurement of agonist and antagonist ligand binding parameters at the human parathyroid hormone type 1 receptor: evaluation

of receptor states and modulation by guanine nucleotide. J Pharmacol Exp Ther 289:1323–1333
16. Dean T, Linglart A, Mahon MJ, Bastepe M, Juppner H, Potts Jr JT, Gardella TJ 2006 Mechanisms of ligand binding to the PTH/PTHrp receptor: selectivity of a modified PTH(1–15) radioligand for GαS-coupled receptor conformations. Mol Endocrinol 20:931–942
17. Hoare SR, Sullivan SK, Pahuja A, Ling N, Crowe PD, Grigoriadis DE 2003 Conformational states of the corticotropin releasing factor 1 (CRF1) receptor: detection, and pharmacological evaluation by peptide ligands. Peptides 24:1881–1897
18. Kenakin T 2004 Principles: receptor theory in pharmacology. Trends Pharmacol Sci 25:186–192
19. De Lean A, Stadel J, Lefkowitz R 1980 A ternary complex model explains the agonist-specific binding properties of the adenylate cyclase-coupled β-adrenergic receptor. J Biol Chem 255:7108–7117
20. Gardella TJ, Luck MD, Wilson AK, Keutmann HT, Nussbaum SR, Potts JT J, Kronenberg HM 1995 Parathyroid hormone (PTH)-PTH-related peptide hybrid peptides reveal functional interactions between the 1–14 and 15–34 domains of the ligand. J Biol Chem 270:6584–6588
21. Gardella T, Luck M, Jensen G, Usdin T, Jüppner H 1996 Converting parathyroid hormone-related peptide (PTHrP) into a potent PTH-2 receptor agonist. J Biol Chem 271: 19888–19893
22. Behar V, Nakamoto C, Greenberg Z, Bisello A, Suva LJ, Rosenblatt M, Chorev M 1996 Histidine at position 5 is the specificity "switch" between two parathyroid hormone receptor subtypes. Endocrinology 137:4217–4224
23. Dean T, Khatri A, Potetinova Z, Willick G, Gardella TJ 2006 Role of amino acid side chains in region 17–31 of parathyroid hormone (PTH) in binding to the PTH receptor. J Biol Chem 281:32485–32495
24. Berlot CH 2002 A highly effective dominant negative αs construct containing mutations that affect distinct functions inhibits multiple Gs-coupled receptor signaling pathways. J Biol Chem 277:21080–21085
25. Vilardaga JP, Bunemann M, Krasel C, Castro M, Lohse MJ 2003 Measurement of the millisecond activation switch of G protein-coupled receptors in living cells. Nat Biotechnol 21:807–812
26. Rodbell M 1997 The complex regulation of receptor-coupled G-proteins. Adv Enzyme Regul 37:427–435
27. Heck M, Hofmann KP 2001 Maximal rate and nucleotide dependence of rhodopsin-catalyzed transducin activation: initial rate analysis based on a double displacement mechanism. J Biol Chem 276:10000–10009
28. Okazaki M, Nagai S, Dean T, Potts JJ, Gardella T 2007 Analysis of PTH-PTH receptor interaction mechanisms using a new, long-acting PTH(1–28) analog reveals selective binding to distinct PTH receptor conformations and biological consequences in vivo. J Bone Miner Res 22(Suppl 1):1190 (Abstract)
29. Nagai S, Okazaki M, Potts JJ, Juppner H, Gardella T 2007 Dissection of the mechanisms of PTH-mediated inhibition of sodium-dependent phosphate transport using a long-acting PTH(1–28) analog. J Bone Miner Res 22(Suppl 1):1189 (Abstract)
30. Tawfeek HA, Qian F, Abou-Samra AB 2002 Phosphorylation of the receptor for PTH and PTHrP is required for internalization and regulates receptor signaling. Mol Endocrinol 16:1–13
31. Castro M, Dicker F, Vilardaga JP, Krasel C, Bernhardt M, Lohse MJ 2002 Dual regulation of the parathyroid hormone (PTH)/PTH-related peptide receptor signaling by protein kinase C and β-arrestins. Endocrinology 143: 3854–3865
32. Chauvin S, Bencsik M, Bambino T, Nissenson RA 2002 Parathyroid hormone receptor recycling: role of receptor dephosphorylation and β-arrestin. Mol Endocrinol 16: 2720–2732
33. Bisello A, Chorev M, Rosenblatt M, Monticelli L, Mierke DF, Ferrari SL 2002 Selective ligand-induced stabilization of active and desensitized parathyroid hormone type 1 receptor conformations. J Biol Chem 277: 38524–38530
34. Hilton JM, Dowton M, Houssami S, Sexton PM 2000 Identification of key components in the irreversibility of salmon calcitonin binding to calcitonin receptors. J Endocrinol 166:213–226
35. Post SR, Miyazaki H, Tager HS 1992 Identification of a Mg^{2+}- and guanyl nucleotide-dependent glucagon receptor cycle by use of permeabilized canine hepatocytes. J Biol Chem 267:25776–25785
36. Chen X, Macica CM, Dreyer BE, Hammond VE, Hens JR, Philbrick WM, Broadus AE 2006 Initial characterization of PTH-related protein gene-driven lacZ expression in the mouse. J Bone Miner Res 21:113–123
37. Shimizu M, Carter P, Khatri A, Potts JJ, Gardella T 2001 Enhanced activity in parathyroid hormone (1–14) and (1–11): novel peptides for probing the ligand-receptor interaction. Endocrinology 142:3068–3074
38. Shimizu N, Guo J, Gardella T 2001 Parathyroid hormone (1–14) and (1–11) analogs conformationally constrained by α-aminoisobutyric acid mediate full agonist responses via the juxtamembrane region of the PTH 1 receptor. J Biol Chem 276:49003–49012
39. Takasu H, Guo J, Bringhurst F 1999 Dual signaling and ligand selectivity of the human PTH/PTHrP receptor. J Bone Miner Res 14:11–20
40. Majeska RJ, Rodan SB, Rodan GA 1980 Parathyroid hormone-responsive clonal cell lines from rat osteosarcoma. Endocrinology 107:1494–1503
41. Yamamoto I, Shigeno C, Potts JTJ, Segre GV 1988 Characterization and agonist-induced down-regulation of parathyroid hormone receptors in clonal rat osteosarcoma cells. Endocrinology 122:1208–1217
42. Tawfeek H, Abou-Samra A 1999 Over-expression of β-arrestin-2 in LLCPK-1 cells stably expressing a green fluorescent protein-tagged PTH/PTHrP receptor increases internalization. J Bone Miner Res 14(Suppl): SU444 (Abstract)

Molecular Endocrinology **is published monthly by The Endocrine Society (http://www.endo-society.org), the foremost professional society serving the endocrine community.**